Available online at www.sciencedirect.com

ScienceDirect

Advances in Space Research 54 (2014) 1974–1984

ADVANCES IN SPACE RESEARCH (a COSPAR publication)

www.elsevier.com/locate/asr

Alpha Particle X-Ray Spectrometer (APXS) on-board Chandrayaan-2 rover

M. Shanmugam [a], S.V.S. Murty [a,*], Y.B. Acharya [a], S.K. Goyal [a], Arpit R. Patel [a], Bhumi Shah [a], A.K. Hait [b], Aditya Patinge [b], D. Subrahmanyam [b]

[a] PLANEX, Physical Research Laboratory, Ahmedabad 380009, India
[b] Space Application Centre, Ahmedabad 380015, India

Available online 16 March 2013

Abstract

Alpha Particle X-ray Spectrometer (APXS) payload configuration for Chandrayaan-2 rover has been completed recently and fabrication of mechanical assembly, PCB layout design and fabrication are in progress. Here we present the design and performance evaluation of various subsystems developed for APXS payload. The low energy threshold of <1 keV and the energy resolution of ~150 eV at 5.9 keV, for the Silicon Drift Detector (SDD), as measured from the developed APXS electronics is comparable to the standard spectrometers available off-the-shelf. We have also carried out experiments for measuring fluorescent X-ray spectrum from various standard samples from the USGS catalog irradiated by the laboratory X-ray source ^{241}Am with 1 mCi activity. It is shown that intensities of various characteristic X-ray lines are well correlated with the respective elemental concentrations.

Keywords: Alpha Particle X-ray Spectrometer; Silicon Drift Detector; CSPA; X-ray spectrometer

1. Introduction

Alpha Particle X-ray Spectrometer (APXS) is a well proven instrument for quantitative elemental analysis of the planetary surfaces through in situ measurements. Measuring the elemental composition of planetary bodies, particularly the major surface constituent elements such as Mg, Al, Si, Ca, Ti and Fe is very important as it can constrain various theoretical/phenomenological models of the origin and evaluation of the respective bodies. Several Mars missions such as Mars Path Finder (MPF) (Rieder et al., 1997), Mars Exploration Rover (MER) (Rieder et al., 2003) and Mars Science Lab (MSL) (Gellert et al., 2009) have carried APXS instruments onboard. APXS instrument onboard MPF and MER have provided elemental composition for several surface samples. APXS onboard MSL is an improved version of APXS flown on MER and is presently operational. The comet mission Rosetta is also carrying APXS onboard PHILAE Lander (Klingelhofer et al., 2007) which is expected to reach the comet 67P/Churyumov–Gerasimenko in the year 2014. Several recent lunar orbiting missions such as Smart-1 (Grande, 2001), Kaguya-Selene (Ogawa et al., 2008), Chandrayaan-1 (Grande et al., 2009) have carried large area X-ray spectrometers for global elemental composition measurements through remote sensing and have provided useful elemental composition information at larger spatial scale. So far, APXS instrument has not been flown on the Moon for surface elemental composition studies. Chandrayaan-2, the second Indian lunar mission having Orbiter, Lander and Rover, slated for launch in 2013–2014, gives us unique opportunity to plan such instrument to carry out the in situ elemental composition measurements.

In-situ measurements on the Moon have been initiated in late 1960s through detection of back scattered alpha particles with Surveyor Lander program on Moon (Turkevich et al., 1967). Though lack of atmosphere on Moon offers an

* Corresponding author. Tel.: +91 9099021758; fax: +91 7926314407.
E-mail address: murty@prl.res.in (S.V.S. Murty).

0273-1177/$36.00 © 2013 COSPAR. Published by Elsevier Ltd. All rights reserved.
http://dx.doi.org/10.1016/j.asr.2013.03.011

advantage in terms of the absence of attenuation of alphas and X-rays, the fluffy regolith and temperature extremes offer new challenges for the operation of APXS on lunar rovers. The landing site of Chandrayaan-2 is yet to be finalized, though it is likely to be south polar sunlit region, where the temperature excursions are expected to be in the range of -30 to -190 °C (day/night) (Paige et al., 2010). As compared to Mars, the environment on Moon is under very high vacuum and also experiences temperature extreams during day/night cycles. Though high vacuum provides an advantage in preventing absorption losses of alphas and X-rays, the temperature extremes pose a problem in maintaining the operational conditions and/or survival of the system.

The objective of the APXS experiment onboard Chandrayaan-2 is to analyse several soil/rock samples along the rover track for the major elements composition in the high latitude polar region. This is the first time such measurement will be carried out on the Moon. The plan is to image the Moon samples to be measured using navigation and imaging cameras onboard rover and traverse the rover towards the sample to carry out the fluorescence measurement using APXS instrument. This will be repeated for several lunar samples during the rover life time. Here we report the design and development of laboratory model of APXS instrument with performance results.

2. Working principle

APXS involves the measurement of characteristic X-rays emitted from the lunar surface due to alpha Particle Induced X-ray Emission (PIXE) and X-ray Florescence (XRF) processes, both alphas and X-rays being emitted by a radioactive source. The ^{244}Cm source has been chosen for the present APXS experiment which emits both alpha particles (5.8 MeV) and X-rays with energies of 14.3 and 18.4 keV. It is well known that the PIXE is dominant for low Z elements (Rieder et al., 2003) while XRF is more prominent for high Z elements, allowing the determination of elements from Na to Br, spanning the energy range of 0.9–25 keV, for the Kα X-rays. We use six alpha sources, each with activity of $\sim 5 \pm 25\%$ mCi (total activity of about 30 mCi). Each source is an 8 mm circular disc with <1 mm thickness having 6 mm active spot at the center. These sources are coated on Si substrate (Radchenko and Ryabinin, 2010) and sealed with 3 μm thick light tight titanium (Ti) foil. The source configuration is similar to flight sources used on Mars Exploration Rover missions.

3. Instrument configuration

In an earlier configuration, APXS has been configured to have two packages, the sensor head, mounted on a robotic arm to give greater flexibility for maneuvering the approach to samples, and an electronics package on the rover chassis (Shanmugam et al., 2011). Presently, APXS instrument is configured as a single package and mounted in the front side beneath the rover chassis due to mass constraint. The exploded view of APXS payload assembly is shown in Fig. 1. APXS payload is placed at a height of 180 mm from the lunar surface. APXS is positioned between the two navigation cameras mounted in the front side of the rover. The APXS package consists of a SDD detector mounted on the source holder along with the six alpha sources in the periphery of the assembly. The sources are collimated such that they view maximum common sample area covering about 220 mm diameter from the height of 180 mm and the same area is viewed by the detector. The assembly also consists of stack of three PCBs for detector signal readout (design details described in Section 5) and shutter with motor to protect the detector and sources from lunar dust. The shutter is positioned close to the circular periphery of the source holder with minimum gap of <1 mm. The inner side of the shutter will be coated with desired material of known chemical composition for APXS instrument calibration as and when desired. Representation of one such mounting view of APXS is shown in Fig. 2.

The APXS instrument configuration described in this section has been finalized recently and design, fabrications of the various parts are in progress. The suitable motor required for the shutter mechanism has been identified and design & testing of the same is in progress. In this

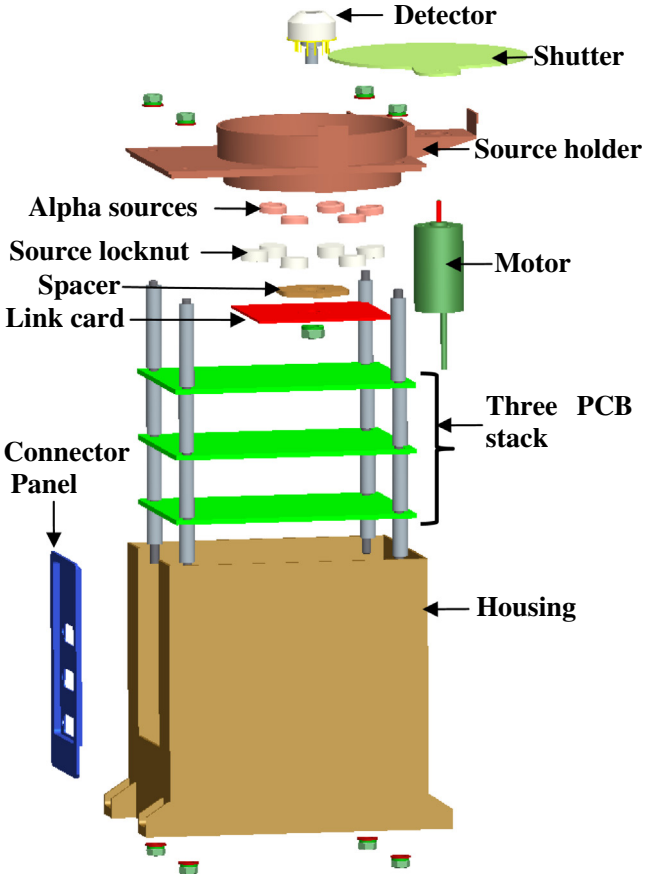

Fig. 1. Exploded view of APXS payload showing various assemblies.

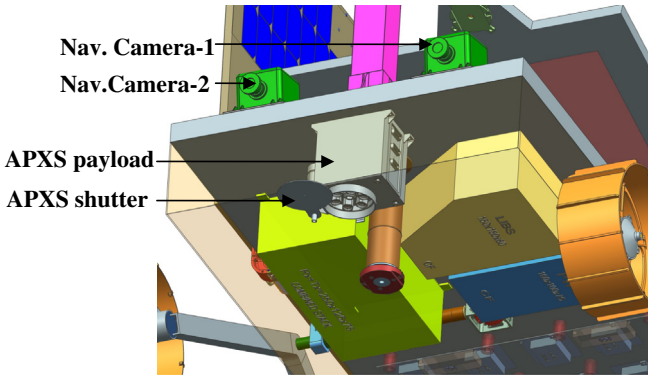

Fig. 2. APXS mounting position on the rover.

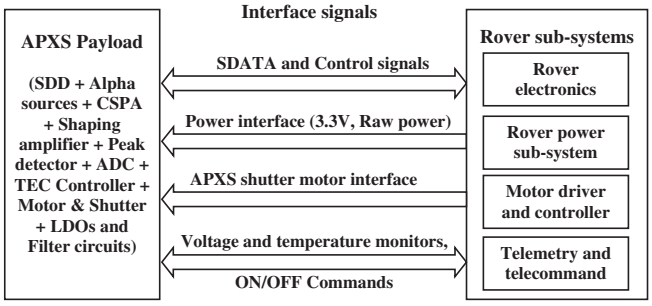

Fig. 3. Block schematic showing APXS interface with rover.

paper, we present the laboratory developments carried out for the APXS payload with performance results obtained from the laboratory setup.

To minimize the overall power and mass requirement of the rover and the payloads on the rover, it is planned to share various resources from the rover for APXS payload such as power, Field Programmable Gate Array (FPGA) based control & data acquisition system and the shutter motor driver. However, for laboratory check out purpose, these systems are independently developed. The interface block schematic of the APXS payload with rover is shown in Fig. 3. The APXS instrument configuration planned for Chandrayaan-2 rover is compared with the instruments flown in MER and MSL as shown in Table 1.

4. Detector selection

The choice of detector for APXS experiment covering the energy range of 1–25 keV with high energy resolution essentially comes to thick Silicon based detector. This Si detector can be availed in different electrode configurations, either as plain Si-PIN detector or as Silicon Drift Detector (SDD). We choose SDD for APXS experiment due to its superior performance compared to Si-PIN of same area. SDD is functionally similar to a Si-PIN photodiode but has different electrode structure as shown in Fig. 4, which results in very low detector capacitance and therefore, under similar operating conditions, the SDD gives better energy resolution than a Si-PIN diode of same size. Table 2 gives comparison of SDD and Si-PIN detectors of same size. The SDD concept was first introduced by Gatti and Rehak (1984) and the first circular SDD,

Table 1
Comparison of APXS instrument configurations.

Parameters	MER	MSL	Chandrayaan-2
Detector (area)	SDD (10 mm^2)	SDD (10 mm^2)	SDD (30 mm^2)
Source activity	30 mCi, ^{244}Cm	30 mCi of conventional sealed ^{244}Cm and 30 mCi of alpha emitting ^{244}Cm	30 mCi, ^{244}Cm
Detector-sample distance	30 mm	<20 mm	~180 mm
Sample diameter	38 mm	17 mm	220 mm
Resolution at 5.9 keV	180 eV	155 eV	150 eV
Low energy threshold	1 keV	0.7 keV	0.6 keV

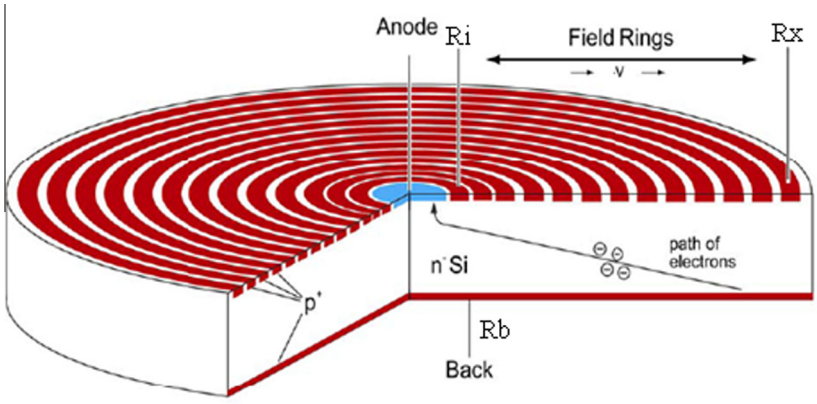

Fig. 4. SDD electrode configuration (Courtesy KETEK, GmbH).

Table 2
Comparison of SDD and Si PIN detectors.

Properties	Silicon Drift Detector (SDD)	Si PIN detector
Detector area/thickness	~20mm^2/500 μm	~20mm^2/500 μm
Detector capacitance	~50 fF	~4 pF
Resolution (peaking time 3 μs)	~150 eV	~300 eV
Peak/background ratio[a]	8200/1	2000/1

[a] http://www.amptek.com/xrselect.html.

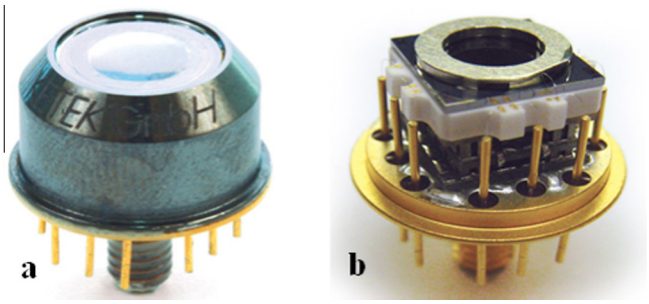

Fig. 5. Photographic view of a SDD module, (a) Enclosed SDD module (b) Internal view (Courtesy KETEK, GmbH).

optimized for energy measurements was described by Rehak et al. (1985). The early SDDs require drift rings in both sides, but in 1987, Kemmer et al. (1987) introduced a design using a planar contact on one side with drift rings on the opposite side. SDD detectors with such contacts are commercially available for various applications and the research still continues for further improvements (Carini and Chen, 2009; Zampa et al., 2009).

The SDD used in APXS experiment has an active area of 30 mm^2 with thickness of 450 μm and is procured from KETEK, GmbH. These SDDs are available in the form of integrated modules, which contain SDD, JFET, charge integration (feedback) capacitor, reset diode, temperature sensor diode and Peltier cooler (internal electrical interconnection given at http://www.ketek.net/products/vitus-sdd/). One such detector module from KETEK, GmbH is shown in Fig. 5. In recent years, SDDs are fabricated with N-channel JFET in the silicon substrate which yields an improvement in energy resolution (Pinotti et al., 1993). These SDD modules provide good energy resolution when the SDD chip is cooled to temperature $\leqslant -35$ °C (KETEK_VITUS_H30_Datasheet_Rev06.07.2009.pdf) which can be achieved by applying suitable power to the inbuilt Peltier cooler.

5. APXS instrument design

In recent years, the laboratory X-ray spectrometers which combine full functionality in a small single package are available (http://www.ketek.net/products/axas/axas-d/, http://www.amptek.com/x123sdd.html etc.). However these are designed for ground based applications and not suitable for space use. Instruments developed for space/planetary exploration need to be configured based on the scientific requirement and other mission constrains. It also should use space worthy components and such instruments are not available readily off-the-shelf. Hence it is required to design and develop individual sub-systems using space worthy components as per the scientific requirement. In this direction, all the sub-systems for the APXS spectrometer have been developed using space qualified components and tested for performance characteristics. The block schematic of the APXS instrument design is shown in Fig. 6.

APXS instrument design involves front-end charge readout system from the SDD detector and then converting into digital form. The design also involves high voltage bias generation for the detector charge collection and Peltier controller design for maintaining the stable detector temperature during its operation. The analog front-end readout system is called APXS electronics, which gives 12 bit serial digital data for every X-ray interacting with the detector to the digital readout system. The digital readout system is part of rover electronics shared by the APXS payload. For ground testing and calibration of the APXS payload, we have also developed APXS readout system which is functionally similar to the rover readout system.

APXS electronics consists of SDD module coupled with Charge Sensitive Pre-Amplifier (CSPA) for charge to voltage conversion followed by shaping amplifier, Peak detector and A/D converter. APXS electronics also consists of high voltage bias generator for charge collection and Peltier controller for maintaining the stable detector temperature. The event trigger generator provides reference to activate the digital controls and process required for data collection. The APXS readout system is a Field Programmable Gate Array (FPGA) based digital readout system which controls peak detection, A/D conversion and storage of the data in the prescribed packet format. For the purpose of ground testing and calibration, the FPGA based digital readout system has been interfaced with Peripheral Component Interface (PCI) and personal computer using LABVIEW software. The LABVIEW software plots the spectral data acquired from the FPGA. Design of individual subsystems is described in the following subtopics.

5.1. Charge Sensitive Pre-Amplifier (CSPA)

Charge Sensitive Pre-Amplifier (CSPA) is widely used in radiation spectroscopy. The charge carriers induced in the active volume of the detector due to photo electric effect is collected by applying suitable high voltage bias to the electrodes of the detector. These charge clouds are then converted into voltage pulses by using CSPA. There are two types of CSPAs, one is “RC feedback type” and another is “Reset type”. The internal configuration (described at http://www.ketek.net/products/viamp/) of the SDD module is compatible with only “Reset type” pre-amplifier.

The CSPA has been developed using high frequency, wide bandwidth and high slew rate video amplifier ICs with first stage containing charge to voltage conversion followed

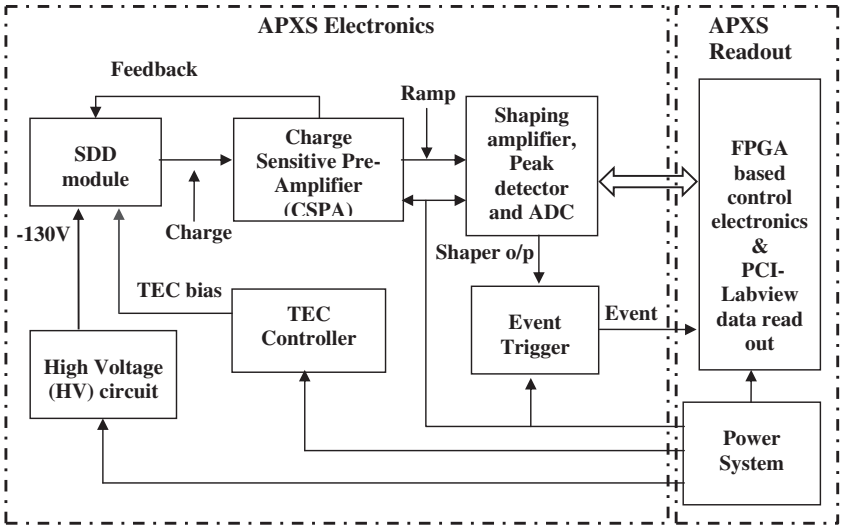

Fig. 6. Block schematic of APXS payload design.

by a gain amplifier. The output of the charge to voltage conversion amplifier is in the form of a ramp signal consisting of small steps (few millivolts/step) and each step in the ramp indicating X-ray interacting with the detector and height of the step gives energy of the X-ray photon. The sensitivity of the charge to voltage conversion amplifier is about 0.9 mV/keV for the feedback capacitor value of 50 fF inside the SDD module. The gain amplifier provides gain of ~5 and the output of the gain amplifier is fed to a comparator based reset pulse generator circuit which provides reset pulses of ~1 μs duration on detecting the set ramp threshold (Fiorini and Lechner, 2002) to discharge the feedback capacitor. The ramp signal frequency depends on the detector leakage current in the absence of X-ray interaction and varies with energy and rate of X-ray interacting with the detector. CRO screen shot of one such ramp signal and steps in the ramp is shown in Fig. 7.

In recent years, promising results in the SDD readout technology with low noise, multi-channel Application Specific Integrated Circuit (ASIC) have been reported (Fiorini et al., 2007; Frizzi et al., 2007), but its suitability and availability for the space use is not known. There are recent developments aimed at integrating a single channel CMOS ASIC based CSPA inside the SDD module (Bombelli et al., 2010) which show that the performances of such SDD modules are better than SDD modules with inbuilt JFET device. These SDD modules are not yet available commercially and hence we have developed discrete component based CSPA for the detector readout.

5.2. Shaping amplifier

The step pulses from the CSPA needs to be amplified with optimal pulse peaking time for the improved energy resolution. The shaping amplifier has been designed with low noise, high speed and wide bandwidth amplifier ICs consisting of three stage CR-$(RC)^2$ type (5 pole) shaping. The first stage of the shaping amplifier consists of CR- high pass filter (differentiator) with provision for pole-zero compensation followed by an amplifier having gain of 5. The second & third stages of the shaping amplifier consist of RC-low pass filters (integrator) and amplifiers having gain

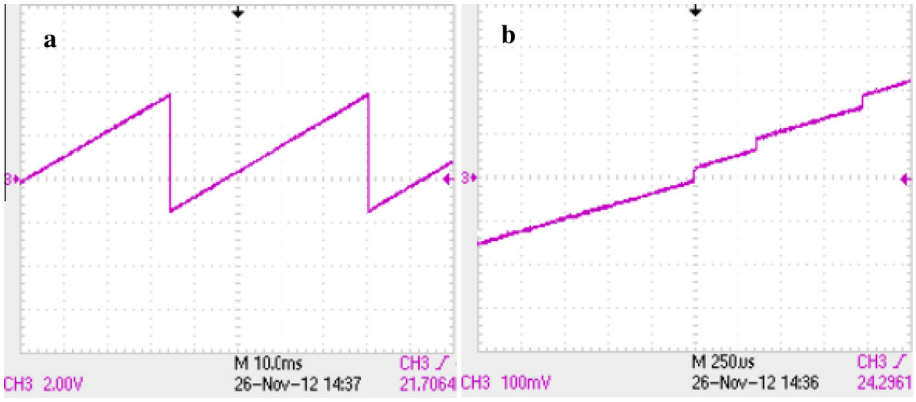

Fig. 7. (a) CRO screen shot of ramp signal output from CSPA, (b) CRO screen shot of step on the ramp signal indicating X-ray interaction with the SDD detector.

of 5 and 3 respectively. The three stage shaping amplifier provides the total gain of about 75 such that the pulse signal amplitudes are maintained within 2.5 V (A/D converter input range) for the maximum X-ray energy of about 25 keV.

5.3. Event triggers generator, Peak detector and A/D conversion

The shaping amplifier output is passed through the event trigger generator circuit to generate digital pulses for each X-ray interacting with the detector to initiate the digital readout system for event data processing. This is carried out by using a fast voltage comparator which provides an output pulse when the input signal amplitude crosses the set threshold. The threshold level of the comparator will be fixed well above the noise level in the flight model based on the ground calibration for certain range of temperatures. Variable threshold through ground command is not planned due to the overall resource constraints on the rover. The shaping amplifier output is also provided to a peak detector which holds the pulse peak voltage for the duration of analog to digital conversion and pulse processing. The used AMPTEK PH300 peak detector is available in hybrid form as a single package which consumes low power with low droop rate. The control logic is designed such that the peak detector holds the analog pulses for the duration of 40 μs which include analog to digital conversion and serial data readout. We have used 12 bit serial analog to digital converter in this experiment which has throughput rate of 8 MHz. The analog to digital converter is successive approximation type with conversion time of 6 μs and requires external reference voltage of 2.5 V. The serial data from the ADC is read using 500 kHz serial burst clock from the digital readout system as planned in the rover readout.

5.4. High voltage bias requirement for SDD

The induced charge carriers in the active volume of the SDD are collected to a point anode by applying High Voltage (HV) biases to Rx (outer ring), Ri (inner ring) and Rb (back contact) with voltage levels of −130 V, −20 V and −60 V respectively. These voltage levels have been generated using HVM make nHV0502N module which is low power device with mass of 2 g. It is a programmable voltage multiplier module proving maximum voltage of −200 V. The programming voltage has been set to obtain the output voltage of about −130 V which is applied to Rx terminal of the SDD and other voltage levels −20 and −60 V required for Ri and Rb contacts are obtained from −130 V using resistive divider network. The total load current requirement on these voltage levels is about ~20 μA. This module consumes less than 100 mW power during SDD operation. Since the module nHV0502N is not space qualified and does not have space heritage, it will be used after it passes various environmental tests.

5.5. Peltier controller

SDD module used in the APXS experiment is provided with two stage inbuilt Peltier cooler to cool the detector chip so as to achieve the best possible energy resolution. The cold side of the peltier is coupled with SDD chip and the hot side of the Peltier cooler is coupled to kovar base plate and then to a M4 screw made of copper for effective heat conduction (as shown in Fig. 5). This metallic portion of the detector is coupled with a 1 mm thick Al assembly (lab test setup) which acts as heat sink to drain out the heat produced by the Peltier cooler. Independent tests showed that the peltier cooler consumes about 1.25 W power to maintain the SDD at −35 °C when the room temperature is 25 °C providing the energy resolution of 150 eV at 5.9 keV.

It is important to maintain the SDD chip at constant temperature during the payload operation independent of ambient temperature variations. Any change in the SDD chip temperature during payload operation will result in energy position shift and degradation in energy resolution. To maintain the SDD chip temperature at −35 °C, we have developed an active Peltier cooling mechanism with PWM technique and it allows the required current through the peltier to get desirable ΔT. It has been tested with detector temperature stability of <1 °C, achieved within two minutes time from power on.

6. APXS readout

APXS readout system is functionally similar to digital readout system being shared by APXS with rover. This readout system is developed for ground testing of APXS payload in mission mode. APXS readout system consists of FPGA based control logic and PCI based PC interface with LABVIEW software for data readout. On occurrence of event trigger pulse, the FPGA provides necessary control signals for the peak detector to hold the signal amplitude and initiates the analog to digital conversion. After 6 μs, the FPGA reads 12 bit serial data by providing serial clock to ADC. The acquired 12 bit serial data is then stored into 2 K × 8 bit packet in the fixed memory size. First 50 bytes of the packet contain the payload header information and the remaining memory is used for storing pulse height information. The photographic view of FPGA based APXS readout system is shown in Fig. 8.

Once the memory is filled, LABVIEW based data readout software in the personal computer acquires the 2 KB data packet and stores it into a file. In the mission mode, 2 KB data packets will be stored in solid state recorders (SSR) on-board rover. The LABVIEW based software also plots the spectral data and updates the spectral window on a computer screen for every acquired data packet. It also has additional capabilities for estimating spectral parameters such as energy resolution (Full Width Half Maximum-FWHM), total counts under the peak, peak position, energy/channel and the system linearity. The PCI bus interface has been

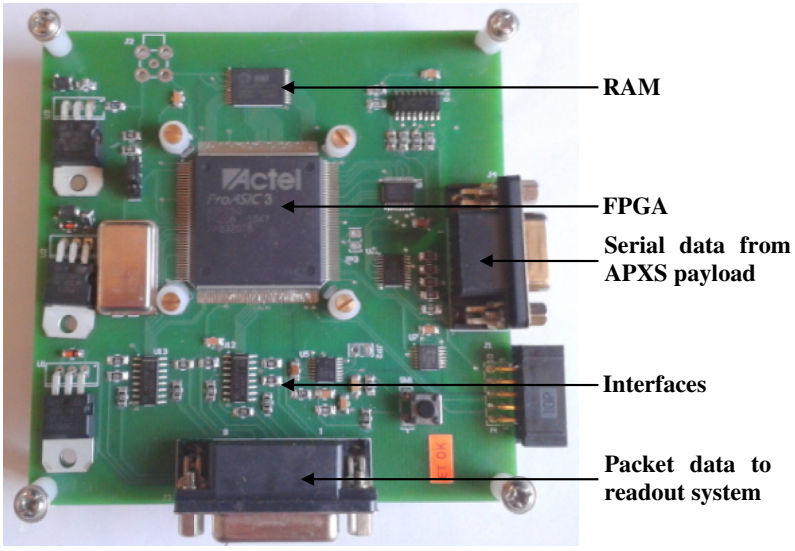

Fig. 8. Photographic view of FPGA based APXS readout system.

established using National Instruments make NI PCI-5364, a 32 bit high speed PCI bus interface.

7. Laboratory experimental setup & system operation

7.1. Laboratory experimental setup

The laboratory experimental setup consists of custom designed Printed Circuit Boards (PCBs) for CSPA, HV and one PCB for shaping amplifier, event trigger, peak detector and ADC. The Silicon Drift Detector is mounted on 1 mm thick Al wall which is part of the experimental setup enclosure. The photographic view of laboratory experimental setup developed for APXS payload is shown in Fig. 9. The SDD is coupled with the Al wall using thermal compound (cho-therm) for the improved heat conduction and the SDD pins are provided with sleeves to isolate from the metallic enclosure. Twelve wires were taken out

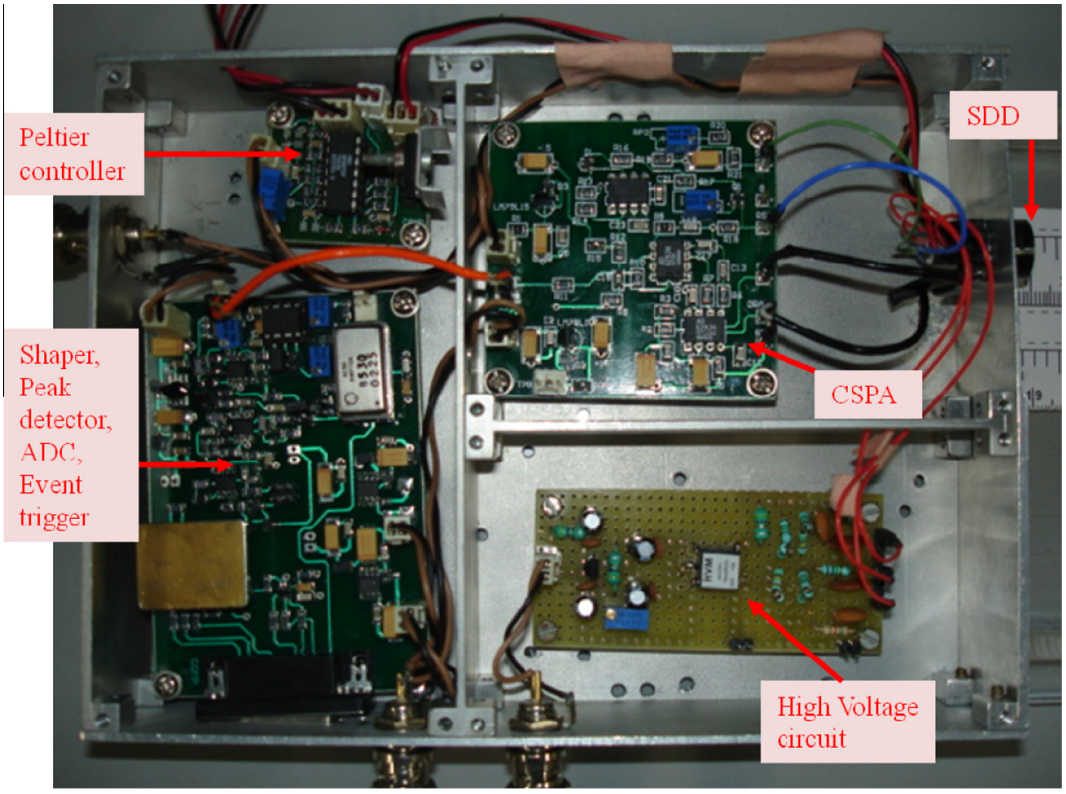

Fig. 9. Laboratory experimental setup developed for APXS payload.

from the SDD pins which have 5 interface lines with CSPA for charge readout, three lines for HV bias, two lines for Peltier power and two lines for chip temperature monitoring. We used shielded cables for charge transfer from SDD to CSPA and also between CSPA & shaping amplifier in the experimental setup to suppress the external noise contribution on the pulsed analog signals. The digital interface is through the APXS readout system.

7.2. System operation

APXS is designed such that the system detects every X-ray event occurring after 40 μs from the previous event and the events occurring within 40 μs are ignored. On occurrence of the event trigger, "Gate" and "Ramp" signals of the peak detector are activated to allow it to charge to the maximum pulse amplitude. Peak detector provides "PKDT" output signal on detecting the pulse peak amplitude indicating that the peak detector is entering into hold mode. Upon detection of "PKDT", the FPGA logic deactivates the "Gate" signal which blocks any subsequent event pulses for the duration of ~40 μs. The ADC starts conversion process on the falling edge of the Gate by activating "Cs_Bar" and the digital data is available after 6 μs. The serial data from the ADC is readout using 500 kHz serial clock frequency generated from the FPGA. It requires 16 clock cycles to readout the 12 bit serial data (Sdata). The data at the serial data output of the ADC is available at the positive edge of the serial clock (Sclk) and the readout system will read the data at the negative edge of the serial clock. Once the serial data is readout, the peak detector is discharged by activating "Ramp" and "Dump" signals for the duration of 1 μs and this process repeats. The overall timing diagram of the system operation is shown in Fig. 10. The FPGA based APXS readout system acquires the serial data and stores it into the memory in the form of 2 KB packets. The LABVIEW based readout software reads packet data stores into a file and also displays the spectra. Software also has the provision to store either event data or spectral data.

8. Results

The sub-systems developed for the APXS payload have been tested for parameters such as spectral energy resolution and X-ray fluorescence detection from different USGS samples with varied elemental concentration. Experimental results are described below.

8.1. Spectral energy resolution

The performance of the sub-systems developed for the APXS experiment has been evaluated using three radioactive sources namely ^{55}Fe (5.9 keV), ^{241}Am (14.1 and 17.9 keV) and ^{109}Cd (22.1 keV) with known X-ray energies. These sources were placed one at a time in front of the detector and the spectra acquired for the total exposures of ~100s from each source. The combined spectral response for three sources is shown in Fig. 11a with energy resolution of about 150 eV at 5.9 keV for detector operating temperature of −35 °C and the pulse peaking time of ~3 μs. The energy resolution of the developed APXS electronics has been compared with the measurements carried out in the standard off-the-shelf SDD based spectrometer

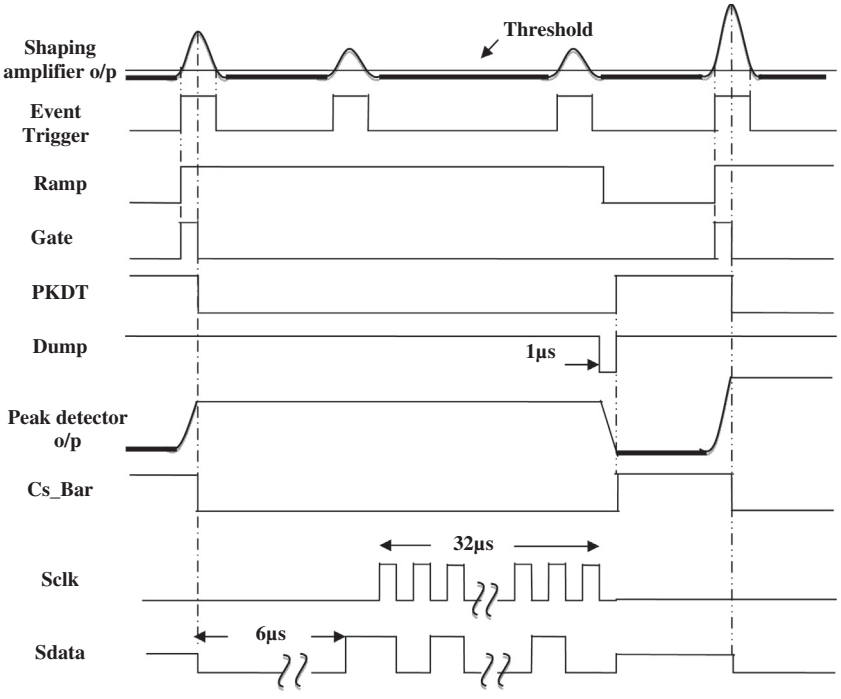

Fig. 10. Timing diagram showing the APXS payload operation.

procured from KETEK, GmbH. The spectral response obtained from this standard spectrometer using the same three sources is shown in Fig. 11b where the detector is cooled to around −40 °C with signal peaking time of 4 μs. The energy resolutions for the four prominent X-ray lines are compared as shown in Table 3. It is shown that the energy resolutions at these energies obtained from the developed APXS electronics is similar to the standard spectrometer.

The SDD detector module used in the experiment provides energy resolution of ~150 eV at 5.9 keV for detector temperatures ⩽−35 °C and the energy resolution degrades for higher detector temperatures (KETEK_VITUS_H30_Datasheet_Rev06.07.2009.pdf). In this direction, we also measured the energy resolution of the system for various detector temperatures by maintaining the ambient temperature at 25 °C. It is shown in Fig. 12 that the energy resolution (150 eV at 5.9 keV) is constant for detector temperatures ⩽−35 °C and degrades to ~320 eV at around 0 °C. It is also observed that the peak energy position shift is non-linear with detector temperature and it changes to ~18 eV at 5.9 keV when the detector temperature changes from −35 °C to −20 °C and ~80 eV for −20–0 °C. We have selected −35 °C as optimum operating temperature for the SDD, for best FWHM.

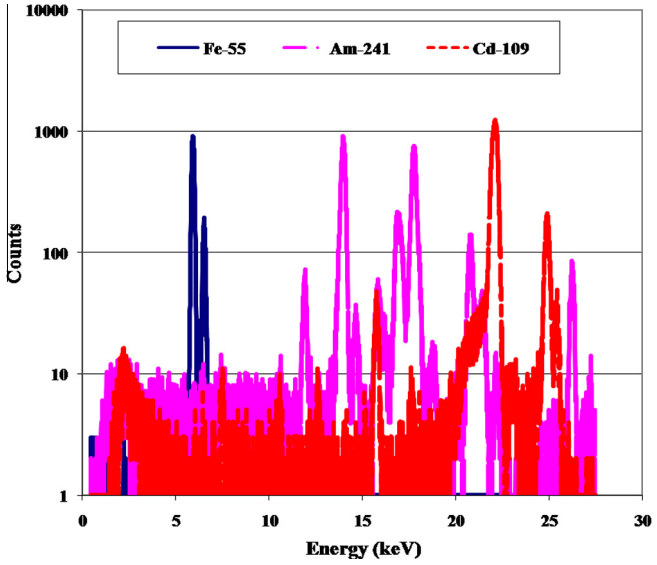

Fig. 11a. Spectra obtained from the developed APXS electronics in the laboratory using three X-ray sources namely Fe-55, Am-241 and Cd-109.

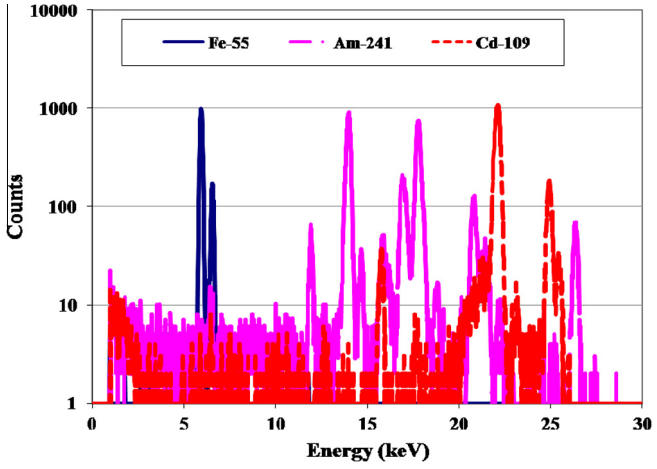

Fig. 11b. Spectra obtained from KETEK make off-the-shelf SDD based X-ray spectrometer using three X-ray sources namely Fe-55, Am-241 and Cd-109.

Table 3
Energy resolution at different X-ray line energies obtained from the developed and standard spectrometer systems.

X-ray line energies	5.9 keV (^{55}Fe)	14.1 keV (^{241}Am)	17.9 keV (^{241}Am)	22.1 keV (^{109}Cd)
Resolution (FWHM) obtained from the developed system (eV)	150	240	269	341
Resolution (FWHM) obtained from the standard system (eV)	143	237	270	336

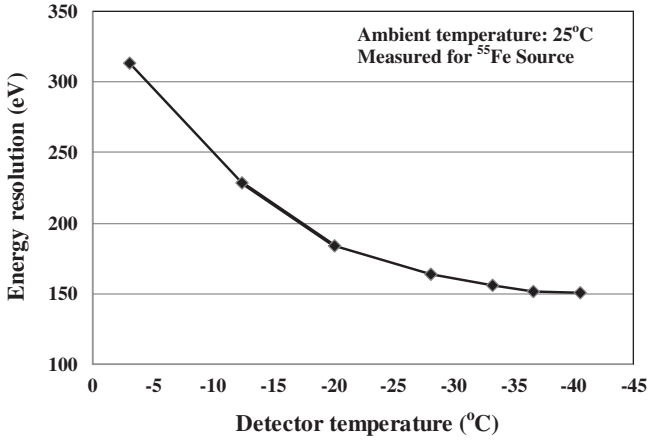

Fig. 12. Energy resolution dependence on SDD detector temperature.

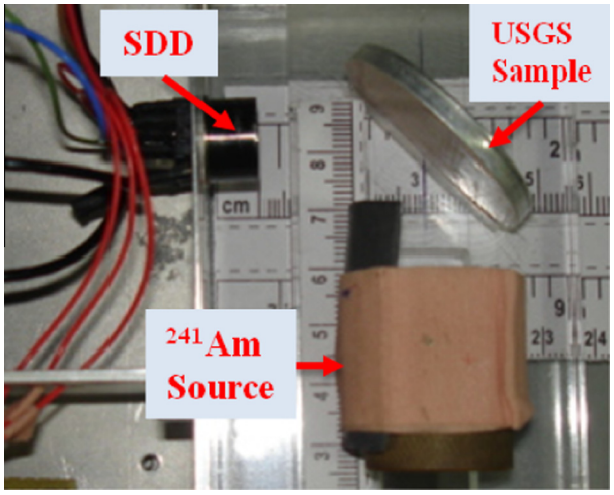

Fig. 13. Sample setup for X-ray florescence measurements.

8.2. Measurement of X-ray fluorescence

We also performed detection of X-ray fluorescence by irradiating some USGS standard samples with the ^{241}Am X-ray source of 1 mCi activity. The sample is positioned such that centers of X-ray source – sample – detector are aligned as shown in Fig. 13. We used several USGS standard samples having different elemental composition for the measurement. The data acquisition was carried out for the duration of 3000 s for each of these USGS samples. Figs. 14a and 14b show the variation in intensity of the characteristic lines for Fe and Ti as a function of their known concentration. It can be seen that there is strong linearity between line intensities and elemental concentration as expected and that these relations can be used to infer concentration of these elements in unknown samples as well. Obviously these linear relations are valid for a given source – sample – detector configuration (used in our experiment only) and any other configuration would require independent calibration, and such work is under progress.

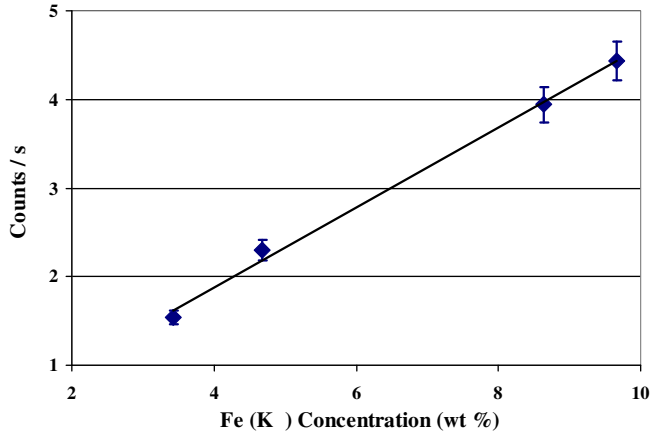

Fig. 14a. Intensity variation of the characteristic X-ray line for Fe as a function of their known concentration (wt%).

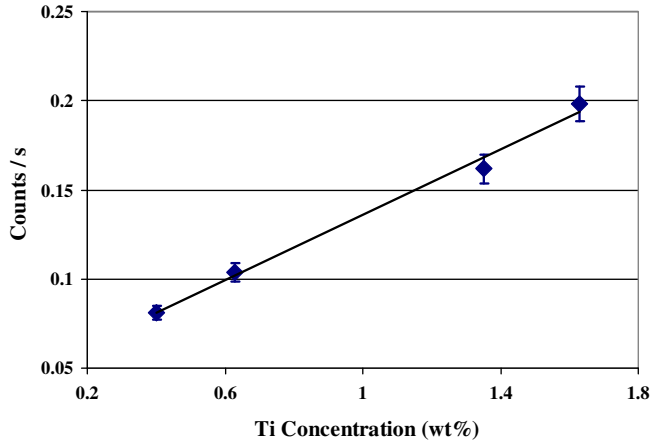

Fig. 14b. Intensity variation of the characteristic X-ray line for Ti as a function of their known concentration (wt%).

9. Conclusions

The developed APXS sub-systems have been tested in the laboratory for functional and performance requirements and it has been shown that the developed APXS system provides energy resolution of about 150 eV at 5.9 keV, which is comparable to standard X-ray spectrometers readily available. We also obtained fluorescence spectra from USGS samples showing that the counts under the Fe and Ti peaks vary linearly with the concentration. The mechanical model of the APXS has been finalized recently after several deliberations and meetings with rover and its subsystem teams. Fabrication of the mechanical model and the design and fabrication of PCBs are in progress to make payload model for laboratory verification. Subsequently, we will complete the Qualification and Flight model of the APXS payloads by mid 2013. The detailed calibration will be carried out on the flight model of the payload.

Acknowledgments

We thank Tinkal Ladia, Ejaz Ahmad and Parth Dave for assistance at various stages of this project. Two anonymous reviewers are thanked for their valuable suggestions. Department of Space, Govt. of India is thanked for providing funds for this project.

References

Bombelli, L., Fiorini, C., Frizzi, T., Nava, R., Greppi, A., Longoni, A. Low-noise CMOS charge preamplifier for X-ray spectroscopy detectors, in: Nuclear Science Symposium Conference Record (NSS/MIC) 2010 IEEE, pp. 135–138, 2010.

Carini, G.A., Chen, W. Performance of a thin-window silicon drift detector X-ray fluorescence spectrometer. IEEE. Trans. Nucl. Sci. 56 (2), 2843–2849, 2009.

Fiorini, C., Frizzi, T., Longoni, A., Porro, M. A CMOS readout circuit for Silicon drift detectors with on-chip JFET and feedback capacitor. IEEE Trans. Nucl. Sci. 53, 2196–2203, 2007.

Fiorini, C., Lechner, P. Charge-sensitive pre-amplifier with continuous reset by means of the gate-to-drain current of the JFET integrated on the detector. IEEE Trans. Nucl. Sci. 49 (3), 1147–1151, 2002.

Frizzi, T., Bombelli, L., Fiorini, C., Longoni, A. The SIDDHARTA chip: a CMOS multi-channel circuit for Silicon drift detectors readout in exotic atoms research. IEEE Nucl. Sci. Symp. Conf. Record N25 (4), 850–856, 2007.

Gatti, E., Rehak, P. Semiconductor drift chamber – an application of a novel charge transport scheme. Nucl. Instr. Methods A 225, 608–614, 1984.

Gellert, R., Campbel, J.L., King, P.L., Leshin, L.A., Lugmair, G.W., Spray, J.G., Squyres, S.W., Yen, A.S. The alpha-particle-x-ray-spectrometer (APXS) for the mars science laboratory (MSL) rover mission, in: Lunar and Planetary Science Conference, abstract no. 2364, 2009.

Grande, M. The D-CIXS X-ray spectrometer on ESA's SMART-1 mission to the Moon. Earth Moon Planets 85, 143–152, 2001.

Grande, M., Maddison, B.J., Sreekumar, P., Huovelin, Johani, Kellett, B.J., Howe, C.J., Crawford, I.A., Smith, D.R. The Chandrayaan-1 X-ray spectrometer. Current Sci. 96 (4), 517–519, 2009.

http://www.amptek.com/xrselect.html.

http://www.amptek.com/x123sdd.html.

http://www.ketek.net/products/vitus-sdd/.

http://www.ketek.net/products/axas/axas-d/.

Kemmer, J., Lutz, G., Beleau, E., Prechtel, U., Welser, W. Low capacity drift diode. Nucl. Instr. Methods A 253, 378–381, 1987.

KETEK_VITUS_H30_Datasheet_Rev06.07.2009.pdf.

Klingelhofer, G., Bruckner, J., Duston, C., Gellert, R., Rieder, R. The Rosetta alpha particle x-ray spectrometer (APXS). Space Sci. Rev. 128, 383–396, 2007.

Ogawa, K., Okada, T., Shirai, K., Kato, M. Numerical estimation of lunar X-ray emission for X-ray spectrometer onboard SELENE. Earth Planets Space 60, 283–292, 2008.

Paige, D.A., Siegler, M.A., Zhang, J.A., Hayne, P.O., Foote, E.J., Bennett, K.A., Vasavada, A.R., Greenhagen, B.T., Schofield, J.T., McCleese, D.J., Foote, M.C., DeJong, E., Bills, B.G., Hartford, W., Murray, B.C., Allen, C.C., Snook, K., Soderblom, L.A., Calcutt, S., Taylor, F.W., Bowles, N.E., Bandfield, J.L., Elphic, R., Ghent, R., Glotch, T.D., Wyatt, M.B., Lucey, P.G. Diviner lunar radiometer observations of cold traps in the Moon's south polar region. Science 330, 479–482, 2010.

Pinotti, E., Brauninger, H., Findeis, N., Gorke, H., Hauff, D., Holl, P., Kemmer, J., Lechner, P., Lutz, G., Kink, W., Meidinger, N., Metzner, G., Predehl, P., Reppin, C., Struder, L., Trumper, J., Zanthier, C.V., Keinziora, E., Staubert, G., Radeka, V., Rehak, P., Bertuccio, G., Gatti, E., Longoni, A., Pullia, A., Sampietro, M. The PN-CCD on chip electronics. Nucl. Instr. Methods A 326, 85–91, 1993.

Radchenko, V.M., Ryabinin, M.A. Research sources of ionizing radiation based on transplutonium elements, IOP Conf. Series. Materials Science and Engineering, doi:http://dx.doi.org/10.1088/1757-899X/9/1/01209, 2010.

Rehak, P., Gatti, E., Longoni, A., Kemmer, J., Holl, P., Klanner, R., Lutz, G., Wylie, W. Semiconductor drift chambers for position and energy measurements. Nucl. Instr. Methods A 235, 224–234, 1985.

Rieder, R., Economou, T., Wanke, H., Turkevich, A., Crisp, J., Bruckner, J., Dreibus, G., McSween Jr, H.Y. The Chemical Composition of Martian Soil and Rocks Returned by the Mobile Alpha Proton X-ray Spectrometer. Preliminary Results From The X-ray Mode, Science 278, 1771–1774, 1997.

Rieder, R., Gellert, R., Bruckner, J., Klingelhofer, G., Dreibus, G., Yen, A., Squyres, S.W. The new Athena alpha particle X-ray spectrometer for the Mars exploration rovers. J. Geophys. Res. 108 (E12), 8066–8078, 2003.

Shanmugam, M., Acharya, Y.B., Goyal, S.K., Murty, S.V.S. Alpha particle X-ray spectrometer (APXS) on-board Chandrayaan-2 rover, in: 42nd Lunar and Planetary Science Conference (1232), 2011.

Turkevich, A.L., Franzgrote, E.J., Patterson, J.H. Chemical analysis of the moon at the surveyor 5 landing site. Science 158, 635–637, 1967.

Zampa, G., Rashevsky, A., Vacchi, A. The X-ray spectroscopic performance of a very large area silicon drift detector. IEEE. Trans. Nucl. Sci. 56 (3), 832–835, 2009.